Clinical, Radiological and Pathological Features of SMARCA4 / BRG1-Deficient Non-Small Cell Lung Carcinomas

Chu-Yun Lou
The First Affiliated Hospital of Zhengzhou University
Hui-Ping Zhao
The First Affiliated Hospital of Zhengzhou University
Hao Lu
The First Affiliated Hospital of Zhengzhou University
Pan Liang
The First Affiliated Hospital of Zhengzhou University
Hong-Yan Zhang
The First Affiliated Hospital of Zhengzhou University
Rui Wang
The First Affiliated Hospital of Zhengzhou University
Ke Tian
The First Affiliated Hospital of Zhengzhou University
Jian-Bo Gao (jianbogao0307@163.com)
The First Affiliated Hospital of Zhengzhou University

Research Article

Keywords: Tomography, X-Ray Computed, Carcinoma, Non-Small-Cell Lung, SMARCA4 protein, human

Posted Date: April 4th, 2022

DOI: https://doi.org/10.21203/rs.3.rs-1509537/v1

Clinical, Radiological and Pathological Features of SMARCA4 / BRG1-Deficient Non-Small Cell Lung Carcinomas

Chu-Yun Lou[1], Hui-Ping Zhao[1], Hao Lu[1], Pan Liang [1], Hong-Yan Zhang [2], Rui Wang, Ke Tian[3], Jian-Bo Gao[1]

[1]Department of Radiology, The First Affiliated Hospital of Zhengzhou University, China
[2]Department of Pathology, The First Affiliated Hospital of Zhengzhou University, China
[3]Department of Nuclear Medicine, The First Affiliated Hospital of Zhengzhou University, China
Corresponding author
Jian-Bo Gao jianbogao0307@163.com

Present address:

1: From the Department of Radiology, The First Affiliated Hospital of Zhengzhou University, No.1 Jianshe East Road, Zhengzhou, China.

2: From the Department of Pathology, The First Affiliated Hospital of Zhengzhou University, No.1 Jianshe East Road, Zhengzhou, China.

3: From the Department of Nuclear Medicine, The First Affiliated Hospital of Zhengzhou University, No.1 Jianshe East Road, Zhengzhou, China.

Abstract

Purpose: *SMARCA4/BRG1*-deficient non-small cell lung carcinomas (SMARCA4-dNSCLCs) are rare and malignant tumors. This study aimed to describe the clinical characteristics, computed tomography (CT) findings, and pathologic features of SMARCA4-dNSCLCs.

Methods: A total of 23 cases of SMARCA4-dNSCLCs with complete medical records, including age, course, the results of main laboratory tests, histopathology, and immunohistochemical characteristics, were retrospectively analyzed from January 2019 to August 2021.

Results: Using a combination of clinical data, CT findings, and pathological findings, SMARCA4-dNSCLCs could be more accurately diagnosed in most cases. Five patients were lost to follow-up. At the end of follow-up, 8 patients died, and the remaining patients were alive at 9–15 months. The incidence rate was similar in the right (n=11) and left (n=12) lungs. Moreover, SMARCA4-dNSCLCs were more likely to be found in the superior lobe (n=14) than in the inferior lobe (n=5) and hilum (n=4), and the median tumor size was 42.83 mm (range: 18.57-70.05 mm). Tumors showed deep, mostly inhomogeneous density with unclear margins in CT images. The lesions' shapes included spinous protuberance (n=20), deep lobulation (n=21), and cystic component (n=13), and their radiodensity values ranged from 29.72 to 57.28 Hounsfield Units. After injection of a contrast material, heterogeneous (n=18) or homogeneous (n=2) enhancement was observed. The peak tumor enhancement was most likely to be observed in the venous phase (n=14). Pleural effusion (n=6), obstructive pneumonia (n=16), and pericardial effusion (n=5) were also detected. Twenty patients demonstrated lymph node involvement. Metastatic locations mainly included the brain (n=6), mediastinum (n=17), bone (n=10), adrenal gland (n=4), and liver (n=3). The primary tumors showed ^{18}F-fluorodeoxyglucose avidity in eight patients who underwent positron emission tomography-CT. All these patients showed *BRG-1* deficiency but AE1/AE3, epithelial membrane antigen, and vimentin positivity. Additionally, these tumors showed different degrees of Ki-67 and programmed death-ligand 1 activities.

Conclusions: Most cases of SMARCA4-dNSCLCs in this study presented with infiltrative masses and heterogeneous densities, and their clinical outcomes were poor. Our findings highlight the importance of the differential diagnosis for SMARCA4-dNSCLCs and the utility of diagnostic imaging prior to histopathological analysis.

Keywords: Tomography, X-Ray Computed, Carcinoma, Non-Small-Cell Lung, SMARCA4 protein· human

Introduction

With the constant advancement in gene detection technology and expanding research, *SMARCA4*-deficient non-small cell lung carcinomas (dNSCLCs) have been recognized as a distinct subset of NSCLCs in recent years . Mutations in *SWI/SNF* components occur in up to 20% of tumors, and *SMARCA4* mutations are the most common . Previous studies have reported 15%–35% of *SMARCA4*-inactivating mutations in NSCLC cell lines, approximately 5%–10% in lung adenocarcinomas, and 6% in lung squamous cell carcinomas . Variations in *SMARCA4* are mainly found in the lung and pancreas, even in epithelial ovarian tumors and endometrial carcinomas. Notably, in somatic cells, *SMARCA4*

mutations can lead to the deficiency of *BRG-1*, which is a tumor suppressor gene located in 19p13, and its deficiency often leads to tumorigenesis. Indeed, *SMARCA4*-deficient undifferentiated tumors are caused by the deficiency of *BRG-1*, which is important for the development of cell proliferation. *BRG-1* may play an anti-cancer role by regulating S-phase transcriptional genes, leading to cell cycle arrest and flat cell morphology.

SMARCA4/BRG1-dNSCLCs were first reported in 2000. SMARCA4-dNSCLCs (NSCLCs with *BRG1* deletion) accounted for only 3-6% of all tumors included in one study, and they were not sensitive to conventional chemotherapy and had a poor prognosis. Moreover, Romero et al. proposed that target agents that regulate epigenomes, such as histone deacetylase inhibitors, histone demethylases, and histone modifiers, could be used as new treatment options for SMARCA4-dNSCLCs .

A few studies have discussed the diagnoses of SMARCA4-dNSCLCs, mostly from the perspective of pathology, and recently, some case reports have analyzed the clinical features of SMARCA4-dNSCLCs. However, there has been little discussion about how to diagnose SMARCA4-dNSCLCs through imaging method, which is a significant diagnostic option. Given the current limited morphological description of SMARCA4-dNSCLCs, this study aimed to determine the characteristics of it from multiple aspects, including radiological assessments. We retrospectively collected data on 23 cases of SMARCA4-dNSCLCs in recent years and analyzed these data from the perspective of CT imaging and other clinical features.

Materials and Methods

Patient Selection

We searched the picture archiving and communication system and the pathology records of our hospital from January 2019 to August 2021. A total of 27 patients were identified as having SMARCA4-dNSCLCs during this time period. We reviewed the clinical data of all patients, including demographics, laboratory findings, and therapies. After excluding the patients whose tumors was occurred in both the lung and pancreas (n=1), primary site was the mediastinum (n=2), and pathology result was SMARCA4-dSCLCs (n=1), the remaining 23 cases with SMARCA4-dNSCLCs were finally included in the study. The study was approved by the Ethics Committee of the First Affiliated Hospital of Zhengzhou University.

Computed Tomography Evaluation

All patients underwent baseline Computed Tomography (CT) examinations, which were performed with different scanners as described below (64 multi-detector row CT scanner; slice thickness: 1.25–3 mm; all images could be reformatted in the axial plane). Two patients underwent chest CT alone without contrast agent administration. Twenty-one patients underwent conventional axial scanning and were administered an intravenous injection of nonionic iohexol. Twelve patients underwent additional examinations of the abdomen with a contrast agent. Moreover, 18F fluorodeoxyglucose positron emission tomography (^{18}F-FDG PET/CT), single-photon emission CT(SPECT) and magnetic resonance imaging (MRI) were performed in 6, 12 and 20 patients, respectively.

Two radiologists with more than 20 years of experience evaluated all the CT images independently. They used digital electronic calipers on transverse scans to measure the longest horizontal axis in the mediastinal window. Tumors with projecting multiple linear features were named spiculated tumors. Other evaluated parameters included the location, shape, and enhancement pattern of tumors, while spiculation length was not calculated inside the tumor. The lesions' axial locations were represented as peripheral if their center was within 20 mm of the interface of the chest wall and lung. Otherwise, the locations were described as central. After the intravenous injection of contrast agent, the enhanced CT images in arterial phase (AP) and venous phase (VP) were obtained with a scanning delay of 30 s and 70 s, respectively. We measure the whole tumor density by manually drawing the regions of interest (ROI) which accounting for about 1 / 2 to 2 / 3 of the tumor parenchyma on each slice of the different phase images. The degree of tumor enhancement, which depended on the CT value, was divided into three categories: mildly enhanced (<20 Hounsfield units [HU]), moderately enhanced (20–40 HU), and obviously enhanced (>40 HU).

All patients were diagnosed according to the TNM staging of lung cancer (8th edition). Lymph node metastases were recognized as lymph nodes with a diameter above 10 mm. SMARCA4-dNSCLCs were staged according to the International Association for the Study of Lung Cancer TNM staging standard. The presence of metastases was identified on CT or MRI (bone, brain, adrenal, liver, and spleen). In addition, the presence of metastases was also defined as avidity on ^{18}F-FDG PET/CT or SPECT. The maximum standardized uptake value (SUVmax) of the whole tumor burden was determined when PET/CT was performed. All imaging findings were compared with biopsy or postoperative pathological findings.

Pathological Evaluation

Five patients underwent radical lobectomy, one patient underwent radioactive seed implantation, and the remaining 18 patients underwent bronchoscopic biopsy. The biopsy samples were each acquired with a diameter of 0.3 cm. The diagnostic criteria for SMARCA4-dNSCLCs were as follows: a vaguely defined large cell carcinoma that was poorly differentiated. All biopsy specimens were stained with hematoxylin and eosin. Additionally, we used an automatic slide-staining system (BenchMark XT, Roche, Basel, Switzerland) for immunohistochemical staining. The antibodies used in this study comprised AE1/AE3, anti-cytokeratin (CK)5/6, anti-CK8/18, anti-napsinA, anti-synaptophysin, anti-thyroid transcription factor-1 (TTF-1), anti-BRG1, anti-programmed death-ligand 1 (PD-L1), anti-P40, and Ki-67 antigen. All antibodies were purchased from DAKO (Glostrup, Denmark).

Results

Patient Characteristics

This study comprised 22 men and 1 woman, with a mean age of 62.7 years (range: 48–82 years). Five patients underwent radical lobectomy, the survival time of the rest case were 11, 12, 12, 15, 15 months, respectively. One patient underwent radioactive seed implantation and was still alive 12 months after implantation. The remaining patients were treated with chemotherapy or immunotherapy. Of these, four patients were lost to follow-up, eight patients died 2–20 months after diagnosis, and only five of them are still alive. The median survival time was 12 months.

Clinical and CT features of these patients were summarized in Tables 1 and 2. Most patients had nonspecific symptoms similar to those of patients with normal lung carcinoma, including a smoking history (22/23, 95.65%), chest pain (4/23, 17.4%), chest tightness (4/23, 17.4%), cough (14/23, 60.9%), hoarseness (1/23,4.34%), and hemoptysis (7/23,30.4%). Laboratory findings revealed that patient 2 was positive for tumor abnormal protein, and patient 3 was positive for carbohydrate antigen 125 (CA125). Before treatment, decreased hemoglobin levels and erythrocyte counts were detected in three patients.

Pathological Features

Cytological analysis revealed that the SMARCA4-dNSCLCs tumor cells showed obvious malignant characteristics. A few scattered tumor cells presented under an optical microscope. The epithelial cells are large and cohesively arranged in compact solid nests, and sheets with

well-defined cellular borders and characteristic eosinophilic to clear cytoplasm. Monotonous epithelioid appearance can be observed in them. The rhabdoid morphology showed undifferentiated epithelioid cells with large vesicular nuclei and eosinophilic eccentric cytoplasm.
Table 3 shows the immunohistochemical features of existing patients. All tumors were diagnosed as BRG-1-deficient tumors (23/23). The tumor had varying degrees of Ki-67 expression, and the tumor cells showed positive staining (23/23) for AE1/AE3, epithelial membrane antigen, and vimentin. The PD-L1 index in two patients was higher than 50% (2/15), whereas four patients had a low expression of PD-L1 (4/15); the remaining patients had a poor expression of PD-L1 (9/15). In addition, the component analysis showed TTF-1 focal positivity in two patients (2/23) and TTF-1 focal negativity in all other patients (21/23). Seven patients expressed SOX2 negative (7/8). The majority of SALL4 expression were negative (9/12).

Image Analysis

Of the 23 patients with SMARCA4-dNSCLCs, only four had a solitary lung primary tumor without any metastases. Twenty patients had lymphatic metastasis, of which mediastinal lymph node metastasis accounted for mostly (18 /23). Distant metastases were found in 15 patients, while the common metastatic sites were the bone (10/23), brain (6/23), adrenal gland (3/23), liver (4/23), and spleen (1/23).

The long-axis diameter of the lesions ranged from 14.16 mm to 92.25 mm. Obstructive pneumonia and atelectasis were found around the entities in 16 patients (16/23). Post-obstructive atelectasis was observed in 16 patients (16/23). In contrast to the general ground-glass opacity (GGO), the diameter of the mass in the lung window and mediastinal window was similar. Calcifications were found in three entities, and the appearance of the spiculation sign was observed in 21 entities (21/23).

The tumor showed mainly inhomogeneous density. In the non-contrast phase, the radiodensity values were 35 to 47 HU. In 21 patients who underwent contrast-enhanced CT, all tumors appeared as heterogeneous enhancements. In the arterial and venous phases, the radiodensity values ranged from 32 to 75 HU and 39 to 77 HU, respectively. The larger masses mostly showed mild enhancement, which was more obvious in the venous phase. Vascular encasement was observed in 16 patients (16/21). In addition, multiple metastases appeared as a uniform enhancement.

Pleural effusion was found on the right side in some patients (6/23). Among them, the primary lesion of one tumor was in the left lobe with right side pleural effusion. In another patient, both sides showed pleural effusions, and the right effusion was more obvious than the left. Peripheral lung cancer occurred on the right side with pleural effusion in our cases(n=4).

The SUV value of the tumor was very high on PET-CT (6/23), ranging from 9.9 to 28.2. Bone metastasis (10/23) was frequently observed. The frequent bone metastasis-prone sites detected by SPECT (n=17) were the sacroiliac joint (4/17), rib (4/17), vertebral body (4/17), sternum (3/17), scapula (2/17), femur (2/17), pelvis (1/17), and frontal bone (1/17).

Discussion

Mutations in *SMARCA4* have been reported frequently in cell lines before. In our study, *SMARCA4* inactivation is likely to be more common in NSCLC tumors than has been reported previously. The neoplasm has the highest incidence of intrapulmonary metastasis and is prone to mediastinal invasion and lymph node metastasis .The tumor caused by *SMARCA4/BRG1* deficiency can occur in different organs of the body, such as the stomach, uterus, and breast. *SMARCA4*-deficient thoracic sarcomas in the mediastinum mainly have lymphatic metastasis, and 52.4% of them have distant metastasis. The frequent metastatic sites are the adrenal gland, lung, bone, and brain, as demonstrated in the present study. Notably, Armon *et al.* reported that *SMARCA4* inactivation often occurs in younger people, whereas the middle-aged and elderly male patients accounted for an absolute proportion in this study. Although the location and type of tumors due to *SMARCA4/BRG-1* deficiency are different, they have similar clinical features, which may further explain the consistency of diseases caused by this gene defect. Almost all patients with *SMARCA4/ BRG-1* deficiency have a long smoking history. However, the family history of diseases caused by *SMARCA4/BRG-1* deficiency has not been reported in previous studies. The only female patient in our sample had no smoking history, but her mother had died of lung cancer. Consistent with our findings, *Yang et al.* indicated that older men with a smoking history and primary tumors in the right lung were more likely to carry *KRAS* mutations ,while lack of BRG1 expression was predominantly detected in adenocarcinomas with KRAS and TP53 co-occurring mutations. These genes might influence the primary location of tumors. Further studies with more data are needed to verify this finding.

SMARCA4 cancer mutations disrupt special enzymological sub-steps, which then leads to varies of dynamic defects in living cells. SMARCA4 surface mutations can also alter the dynamic engagement of chromatin by DNA-binding groove mutants, then break engagement with DNA .

Multiple studies demonstrate that deregulated BRG1 can alter transcriptional programs, to increase foster malignant proliferation genes expression . In support of this view, many preclinical studies have demonstrated that BRG1 inactivation contributes to formation of aggressive and invasive tumors from diverse tissue types. BRG1 losses in NSCLC cells were associated with variations in chromatin structure, including differences in nucleosome positioning and occupancy surrounding transcriptional start sites of disease-relevant genes. BRG1 attenuation contributes to NSCLC aggressiveness by altering nucleosome positioning at a wide range of genes, including key cancer-associated genes.

Indeed, SMARCA4-dNSCLC is an extremely aggressive tumor , and regardless of the TNM stage, patients with SMARCA4-dNSCLC always have poor survival outcomes , and the clinical symptoms mostly have no specificity compared to those of other diseases. However, some patients in our study had clinical features due to organ invasions, such as dizziness and headache, and the prognosis of these patients was usually poorer than that of patients without any without any symptoms caused by distant metastases in our study. Crombé *et al.* also indicated that various secondary diseases caused by tumors were the primary cause of patient death. Therefore, the application of imaging methods to judge whether there is distant metastasis is helpful to evaluate the prognosis of the patient in predicting patient prognosis.

Plasma tumor markers, (i.e., CA125, CYFRA21-1, and neuron-specific enolase) have been used to help diagnose NSCLCs and to assess the treatment efficiency. Patients with SMARCA4-dNSCLCs in our study also showed a combined increase in these indices. Carcinoembryonic antigen (CEA) is an acidic glycoprotein with specific determinants of human embryonic antigen, which is related to its wide distribution and high concentration in epithelial tissues. CEA is more sensitive to adenocarcinoma than to other types of lung cancers. The increase in CEA is also mostly manifested in patients with *SMARCA4*-deficient adenocarcinoma. Although CEA was also detected in *SMARCA4*-deficient squamous carcinoma patients, the number was far less than that in *SMARCA4*-deficient adenocarcinoma patients. There was no specificity in CAl25 and CYFRA21-1 in SMARCA4-dNSCLCs compared with general NSCLCs. Thus, the laboratory test results can only be used as a reference, and cannot become the primary method to identify the disease.

CT can completely reveal the primary lesion, invasion range, lymph node involvement, and distant metastasis. SMARCA4-dNSCLCs have a larger volume (45.25 mm) and are more prone to intrapulmonary metastasis than normal NSCLCs. Unlike the general GGO, the diameters of the masses in the lung and mediastinal window were similar. Most have spiculated margins or ill-defined and irregular contours. In addition, due to the malignant cells along the lung interstitium and differential growth rates within tumors, the entities usually manifests as deep lobation and spinous protuberance, indicating that it is a high-risk, malignant pulmonary mass. All benign forms of calcification patterns were rarely detected

in our sample; this finding further strengthens the current clinical consensus that SMARCA4-dNSCLCs is a highly aggressive disease. Moreover, rapidly growing malignant tumors always tend to encounter necrosis which leads to a lower tumor density. The signal of the lesions was always heterogeneous on CT scans in the arterial and venous phases due to the large cystic areas in these lesions, which could make a strong contrast with the cystic part on contrast-enhanced CT. The peak CT value was usually observed in the venous phase in the opening of the lesion's may due to tumor angiogenesis. Moreover, vascular convergence sign and cavitation were the obvious features of this tumor.

The application of PET-CT and SPECT is also helpful in improving our understanding of SMARCA4-dNSCLCs. In this study, the SUV values ranged from 9.9 to 28.2. Notably, in nodules greater than 10 mm in diameter, PET has a high specificity and sensitivity for the detection of malignancy. However, PET cannot be used to discriminate between other tumors because SCLC, lymphoma, and pulmonary carcinoma also have high metabolic activity.

Recently, chemotherapy has been used for SMARCA4-dNSCLCs, which can appropriately delay disease progress . In this study, almost all patients were treated with chemotherapy, but the efficacy varied from individual to individual. Although NSCLC with *BRG-1* deletion was accompanied by a PD-L1-positive status in a previous study, These above cases were rarely PD-L1 positive; thus, immunotherapy was only used in one patient. In addition, neoadjuvant chemotherapy can also be used in the treatment of this disease. Moreover, few patients reportedly underwent surgery . However, five patients in our study chose surgical treatment, in addition to one person who missed follow-up, the rest of them all had a long survival in our study. None of them had distant metastasis, and the diameter of the observed lesions was shorter than that of the patients who only received chemotherapy. These tumors were shown by pathology to lack of BRG-1expression by pathology. Thus, imaging reveals findings that can provide new insights into the treatment of the disease. We can clearly stage the TNM by imaging, so as to determine whether the patients require surgery, and subsequently formulate an appropriate treatment.

Moreover, both of SMARCA4 d-NSCLS and SMARCA4 Deficiency-thoracic carcinoma (SMARCA4-DTS) are BRG-1 deficiency disease with different prognosis. SMARCA4-DTS show a poorly differentiated morphology with small cell, epithelioid, or rhabdoid phenotype cells with focal expression of at least 2 of CD34, SALL4 and SOX2. On the other hand, SMARCA4-dNSCLCs express negative CD34 and SOX2, which contribute to distinguishing SMARCA4-deficiency disease. Besides, SMARCA4 d-NSCLS always have a nearly negative expression of TTF-1and P40, while two-thirds of them are positive for CK7. In addition, imaging is also a vital method to distinguish them. Most

SMARCA4-DTS are mediastinal and pleural located infiltrative and compressive chest tumors with ill-defined necrotic lymphadenopathies, spreading in retroperitoneum, subclavian, axillar, mediastinum, and cervical regions, and more likely to occur peritoneal metastases.

However, the primary site of SMARCA4-dNSCLCs is in the lung, mostly in the upper lobe. Unlike the multi-compartment infiltrative and compressive extension of SMARCA4-DTS, SMARCA4-dNSCLCs patients mostly demonstrated a rounded solid mass, and no patient with peritoneal metastasis was found in our cases. Therefore, the combination of imaging and pathological examination may further improve the diagnostic accuracy SMARCA4-deficiency disease.

Our study has some limitations. Given the lack of data collected from a large sample, statistical analysis could not be performed. We tried to choose the average density place and avoid the necrotic area when drawing ROI. However, there were still some necrotic foci in the tumor parenchyma that cannot be recognized visually. Due to the inconsistency of methodology, measurement errors would be inevitable. Additionally, screening for BRG-1 deficiency patients were diagnosed recently, we were unable to perform an assessment of the long-term prognosis. Besides that, patients with this disease rarely underwent surgery; therefore, it was difficult to determine by pathology whether they had pleural invasion.

Conclusion

We conclude that SMARCA4-dNSCLCs tend to act as a solid tissue with slightly larger volume and more obvious enhancement in the venous period, accompanied by multiple enlarged lymph nodes in the mediastinum. Currently, pathology still remains the gold standard for the diagnosis of SMARCA4-dNSCLCs. Sequencing technology, which is becoming more frequently used as a diagnostic tool, sometimes fails to detect large genomic deletions. Notably, imaging examination can intuitively observe the degree of tumor infiltration and plays an important role in the treatment regimen. Our study is the first to analyze various imaging features of SMARCA4-dNSCLCs. Due to the high invasiveness of SMARCA4-dNSCLCs, a more detailed and rapid clinical intervention with CT is essential. Combined with laboratory examinations and clinical features, imaging can improve the possibility of diagnosing it and give a completely assessment of patients' accurate diagnosis, and help predict patient prognosis.

Abbreviations

CT Computed Tomography**, MRI** Magnetic resonance imaging, **NSCLCs** Non-small Cell Lung Carcinomas, **AP** Arterial Phase, **VP** Venous Phase, **^{18}F-FDG PET/CT** 18F fluorodeoxyglucose positron emission tomography, **SPECT** Single-photon Emission CT.

Contributions

CL: manuscript preparation, data analysis and literature research. HZ and RW: literature research and data analysis. HL and KT: data collection. HZ: guidance of pathological knowledge. PL: guidance of imaging knowledge. JG: study conception and design, manuscript review and guarantor of integrity of the entire study. All authors have read and approved the final manuscript.

References

Agaimy, A. "The Expanding Family of Smarcb1(Ini1)–Deficient Neoplasia: Implications of Phenotypic, Biological, and Molecular Heterogeneity." [In eng]. *Adv Anat Pathol* 21, no. 6 (Nov 2014): 394–410. https://doi.org/10.1097/pap.0000000000000038.

Agaimy, A., and W. D. Foulkes. "Hereditary Swi/Snf Complex Deficiency Syndromes." [In eng]. *Semin Diagn Pathol* 35, no. 3 (May 2018): 193–98. https://doi.org/10.1053/j.semdp.2018.01.002.

Agaimy, A., F. Fuchs, E. A. Moskalev, H. Sirbu, A. Hartmann, and F. Haller. "Smarca4–Deficient Pulmonary Adenocarcinoma: Clinicopathological, Immunohistochemical, and Molecular Characteristics of a Novel Aggressive Neoplasm with a Consistent Ttf1(Neg)/Ck7(Pos)/Heppar–1(Pos) Immunophenotype." [In eng]. *Virchows Arch* 471, no. 5 (Nov 2017): 599–609. https://doi.org/10.1007/s00428–017–2148–5.

Agaimy, Abbas, Ondrej Daum, Bruno Märkl, Ines Lichtmannegger, Michal Michal, and Arndt Hartmann. "Swi/Snf Complex - Deficient Undifferentiated/Rhabdoid Carcinomas of the Gastrointestinal Tract: A Series of 13 Cases Highlighting Mutually Exclusive Loss of Smarca4 and Smarca2 and Frequent Co–Inactivation of Smarcb1 and Smarca2." *The American Journal of Surgical Pathology* 40, no. 4 (2016): 544–53. https://doi.org/10.1097/pas.0000000000000554. https://journals.lww.com/ajsp/Fulltext/2016/04000/SWI_SNF_Complex_deficient.16.aspx.

Agaimy, Abbas, Deepali Jain, Nasir Uddin, Lisa M. Rooper, and Justin A. Bishop. "Smarca4–Deficient Sinonasal Carcinoma: A Series of 10 Cases Expanding the Genetic Spectrum of Swi/Snf–Driven Sinonasal Malignancies." *The American Journal of Surgical Pathology* 44, no. 5 (2020): 703–10. https://doi.org/10.1097/pas.0000000000001428. https://journals.lww.com/ajsp/Fulltext/2020/05000/SMARCA4_deficient_Sinonasal_Carcinoma__A_Series_of.15.aspx.

Armon, S., P. Hofman, and M. Ilié. "Perspectives and Issues in the Assessment of Smarca4 Deficiency in the Management of Lung Cancer Patients." [In eng]. *Cells*

10, no. 8 (Jul 29 2021). https://doi.org/10.3390/cells10081920.

Chae, E. J., J. W. Song, B. Krauss, K. S. Song, C. W. Lee, H. J. Lee, and J. B. Seo. "Dual-Energy Computed Tomography Characterization of Solitary Pulmonary Nodules." [In eng]. *J Thorac Imaging* 25, no. 4 (Nov 2010): 301-10. https://doi.org/10.1097/RTI.0b013e3181e16232.

"Comprehensive Genomic Characterization of Squamous Cell Lung Cancers." [In eng]. *Nature* 489, no. 7417 (Sep 27 2012): 519-25. https://doi.org/10.1038/nature11404.

"Comprehensive Molecular Profiling of Lung Adenocarcinoma." [In eng]. *Nature* 511, no. 7511 (Jul 31 2014): 543-50. https://doi.org/10.1038/nature13385.

Crombé, A., N. Alberti, N. Villard, F. Pilleul, X. Buy, F. Le Loarer, and M. Kind. "Imaging Features of Smarca4-Deficient Thoracic Sarcomas: A Multi-Centric Study of 21 Patients." [In eng]. *Eur Radiol* 29, no. 9 (Sep 2019): 4730-41. https://doi.org/10.1007/s00330-019-06017-x.

Dagogo-Jack, I., A. B. Schrock, M. Kem, N. Jessop, J. Lee, S. M. Ali, J. S. Ross, *et al*. "Clinicopathologic Characteristics of Brg1-Deficient Nsclc." [In eng]. *J Thorac Oncol* 15, no. 5 (May 2020): 766-76. https://doi.org/10.1016/j.jtho.2020.01.002.

Fernando, T. M., R. Piskol, R. Bainer, E. S. Sokol, S. E. Trabucco, Q. Zhang, H. Trinh, *et al*. "Functional Characterization of Smarca4 Variants Identified by Targeted Exome-Sequencing of 131,668 Cancer Patients." [In eng]. *Nat Commun* 11, no. 1 (Nov 3 2020): 5551. https://doi.org/10.1038/s41467-020-19402-8.

Fuller, C. E. "All Things Rhabdoid and Smarc: An Enigmatic Exploration with Dr. Louis P. Dehner." [In eng]. *Semin Diagn Pathol* 33, no. 6 (Nov 2016): 427-40. https://doi.org/10.1053/j.semdp.2016.08.003.

Gould, M. K., L. Ananth, and P. G. Barnett. "A Clinical Model to Estimate the Pretest Probability of Lung Cancer in Patients with Solitary Pulmonary Nodules." [In eng]. *Chest* 131, no. 2 (Feb 2007): 383-8. https://doi.org/10.1378/chest.06-1261.

Gurney, J. W. "Determining the Likelihood of Malignancy in Solitary Pulmonary Nodules with Bayesian Analysis. Part I. Theory." [In eng]. *Radiology* 186, no. 2 (Feb 1993): 405-13. https://doi.org/10.1148/radiology.186.2.8421743.

Hasbahceci, M., F. U. Malya, E. Kunduz, M. Guzel, N. Unver, and A. Akcakaya. "Use of Serum and Peritoneal Cea and Ca19-9 in Prediction of Peritoneal Dissemination and Survival of Gastric Adenocarcinoma Patients: Are They Prognostic Factors?" [In eng]. *Ann R Coll Surg Engl* 100, no. 4 (Apr 2018): 257-66. https://doi.org/10.1308/rcsann.2018.0011.

Heitzman, E. R., B. Markarian, B. N. Raasch, E. W. Carsky, E. J. Lane, and M. E. Berlow. "Pathways of Tumor Spread through the Lung: Radiologic Correlations with Anatomy and Pathology." [In eng]. *Radiology* 144, no. 1 (Jul 1982): 3-14. https://doi.org/10.1148/radiology.144.1.6283592.

Hodges, H. C., B. Z. Stanton, K. Cermakova, C. Y. Chang, E. L. Miller, J. G. Kirkland, W. L. Ku, *et al*. "Dominant-Negative Smarca4 Mutants Alter the Accessibility Landscape of Tissue-Unrestricted Enhancers." [In eng]. *Nat Struct Mol Biol* 25, no. 1 (Jan 2018): 61-72. https://doi.org/10.1038/s41594-017-0007-3.

Horton, R. K., M. Ahadi, A. J. Gill, S. Said, Z. E. Chen, A. Bakhshwin, M. Nichols, J. R. Goldblum, and R. P. Graham. "Smarca4/Smarca2–Deficient Carcinoma of the Esophagus and Gastroesophageal Junction." [In eng]. *Am J Surg Pathol* 45, no. 3 (Mar 1 2021): 414–20. https://doi.org/10.1097/pas.0000000000001599.

Imielinski, M., A. H. Berger, P. S. Hammerman, B. Hernandez, T. J. Pugh, E. Hodis, J. Cho, *et al*. "Mapping the Hallmarks of Lung Adenocarcinoma with Massively Parallel Sequencing." [In eng]. *Cell* 150, no. 6 (Sep 14 2012): 1107–20. https://doi.org/10.1016/j.cell.2012.08.029.

Jiang, Y., A. L. Turinsky, and M. Brudno. "The Missing Indels: An Estimate of Indel Variation in a Human Genome and Analysis of Factors That Impede Detection." [In eng]. *Nucleic Acids Res* 43, no. 15 (Sep 3 2015): 7217–28. https://doi.org/10.1093/nar/gkv677.

Jin, C., M. Yang, X. Han, H. Chu, Y. Zhang, M. Lu, Z. Wang, *et al*. "Evaluation of the Value of Preoperative Cyfra21–1 in the Diagnosis and Prognosis of Epithelial Ovarian Cancer in Conjunction with Ca125." [In eng]. *J Ovarian Res* 12, no. 1 (Nov 25 2019): 114. https://doi.org/10.1186/s13048–019–0587–0.

Kadoch, C., R. T. Williams, J. P. Calarco, E. L. Miller, C. M. Weber, S. M. Braun, J. L. Pulice, E. J. Chory, and G. R. Crabtree. "Dynamics of Baf–Polycomb Complex Opposition on Heterochromatin in Normal and Oncogenic States." [In eng]. *Nat Genet* 49, no. 2 (Feb 2017): 213–22. https://doi.org/10.1038/ng.3734.

Kolin, David L., Charles M. Quick, Fei Dong, Christopher D.M. Fletcher, Colin J.R. Stewart, Anita Soma, Jason L. Hornick, Marisa R. Nucci, and Brooke E. Howitt. "Smarca4–Deficient Uterine Sarcoma and Undifferentiated Endometrial Carcinoma Are Distinct Clinicopathologic Entities." *The American Journal of Surgical Pathology* 44, no. 2 (2020): 263–70. https://doi.org/10.1097/pas.0000000000001375. https://journals.lww.com/ajsp/Fulltext/2020/02000/SMARCA4_deficient_Uterine_Sarcoma_and.15.aspx.

Krüger–Genge, A., A. Blocki, R. P. Franke, and F. Jung. "Vascular Endothelial Cell Biology: An Update." [In eng]. *Int J Mol Sci* 20, no. 18 (Sep 7 2019). https://doi.org/10.3390/ijms20184411.

Lee, S. Y., M. K. Ju, H. M. Jeon, E. K. Jeong, Y. J. Lee, C. H. Kim, H. G. Park, S. I. Han, and H. S. Kang. "Regulation of Tumor Progression by Programmed Necrosis." [In eng]. *Oxid Med Cell Longev* 2018 (2018): 3537471. https://doi.org/10.1155/2018/3537471.

Matsubara, D., Y. Kishaba, S. Ishikawa, T. Sakatani, S. Oguni, T. Tamura, H. Hoshino, *et al*. "Lung Cancer with Loss of Brg1/Brm, Shows Epithelial Mesenchymal Transition Phenotype and Distinct Histologic and Genetic Features." [In eng]. *Cancer Sci* 104, no. 2 (Feb 2013): 266–73. https://doi.org/10.1111/cas.12065.

Medina, P. P., O. A. Romero, T. Kohno, L. M. Montuenga, R. Pio, J. Yokota, and M. Sanchez–Cespedes. "Frequent Brg1/Smarca4–Inactivating Mutations in Human Lung Cancer Cell Lines." [In eng]. *Hum Mutat* 29, no. 5 (May 2008): 617–22. https://doi.org/10.1002/humu.20730.

Mei, X., X. Zhu, L. Zuo, H. Wu, M. Guo, and C. Liu. "Predictive Significance of Cyfra21–1, Squamous Cell Carcinoma Antigen and Carcinoembryonic Antigen for Lymph Node Metastasis in Patients with Esophageal Squamous Cancer." [In eng]. *Int J Biol Markers* 34, no. 2 (Jun 2019): 200–04.

https://doi.org/10.1177/1724600819847999.

Naito, T., H. Udagawa, S. Umemura, T. Sakai, Y. Zenke, K. Kirita, S. Matsumoto, *et al*. "Non-Small Cell Lung Cancer with Loss of Expression of the Swi/Snf Complex Is Associated with Aggressive Clinicopathological Features, Pd-L1-Positive Status, and High Tumor Mutation Burden." [In eng]. *Lung Cancer* 138 (Dec 2019): 35-42. https://doi.org/10.1016/j.lungcan.2019.10.009.

Nambirajan, A., V. Singh, N. Bhardwaj, S. Mittal, S. Kumar, and D. Jain. "Smarca4/Brg1-Deficient Non-Small Cell Lung Carcinomas: A Case Series and Review of the Literature." [In eng]. *Arch Pathol Lab Med* 145, no. 1 (Jan 1 2021): 90-98. https://doi.org/10.5858/arpa.2019-0633-OA.

Nash, S. V., and J. W. Said. "Gastroenteropancreatic Neuroendocrine Tumors. A Histochemical and Immunohistochemical Study of Epithelial (Keratin Proteins, Carcinoembryonic Antigen) and Neuroendocrine (Neuron-Specific Enolase, Bombesin and Chromogranin) Markers in Foregut, Midgut, and Hindgut Tumors." [In eng]. *Am J Clin Pathol* 86, no. 4 (Oct 1986): 415-22. https://doi.org/10.1093/ajcp/86.4.415.

Neunteufel, W., and G. Breitenecker. "[Immunohistochemical Demonstration of Ca 125, Ca 19-9 and Cea in Normal and Pathologically Changed Adnexa]." [In ger]. *Geburtshilfe Frauenheilkd* 48, no. 5 (May 1988): 334-7. https://doi.org/10.1055/s-2008-1035986. Immunhistochemische Darstellung von CA 125, CA 19-9 und CEA in normalen und pathologisch veränderten Adnexen.

Oike, T., H. Ogiwara, Y. Tominaga, K. Ito, O. Ando, K. Tsuta, T. Mizukami, *et al*. "A Synthetic Lethality-Based Strategy to Treat Cancers Harboring a Genetic Deficiency in the Chromatin Remodeling Factor Brg1." [In eng]. *Cancer Res* 73, no. 17 (Sep 1 2013): 5508-18. https://doi.org/10.1158/0008-5472.Can-12-4593.

Orvis, T., A. Hepperla, V. Walter, S. Song, J. Simon, J. Parker, M. D. Wilkerson, *et al*. "Brg1/Smarca4 Inactivation Promotes Non-Small Cell Lung Cancer Aggressiveness by Altering Chromatin Organization." [In eng]. *Cancer Res* 74, no. 22 (Nov 15 2014): 6486-98. https://doi.org/10.1158/0008-5472.Can-14-0061.

Pan, D., J. Chen, C. Feng, W. Wu, Y. Wang, J. Tong, and D. Zhou. "Preferential Localization of Muc1 Glycoprotein in Exosomes Secreted by Non-Small Cell Lung Carcinoma Cells." [In eng]. *Int J Mol Sci* 20, no. 2 (Jan 14 2019). https://doi.org/10.3390/ijms20020323.

Perret, R., L. Chalabreysse, S. Watson, I. Serre, S. Garcia, F. Forest, V. Yvorel, *et al*. "Smarca4-Deficient Thoracic Sarcomas: Clinicopathologic Study of 30 Cases with an Emphasis on Their Nosology and Differential Diagnoses." [In eng]. *Am J Surg Pathol* 43, no. 4 (Apr 2019): 455-65. https://doi.org/10.1097/pas.0000000000001188.

Rekhtman, N., J. Montecalvo, J. C. Chang, D. Alex, R. N. Ptashkin, N. Ai, J. L. Sauter, *et al*. "Smarca4-Deficient Thoracic Sarcomatoid Tumors Represent Primarily Smoking-Related Undifferentiated Carcinomas Rather Than Primary Thoracic Sarcomas." [In eng]. *J Thorac Oncol* 15, no. 2 (Feb 2020): 231-47.

https://doi.org/10.1016/j.jtho.2019.10.023.

Romero, O. A., A. Vilarrubi, J. J. Alburquerque-Bejar, A. Gomez, A. Andrades, D. Trastulli, E. Pros, *et al.* "Smarca4 Deficient Tumours Are Vulnerable to Kdm6a/Utx and Kdm6b/Jmjd3 Blockade." [In eng]. *Nat Commun* 12, no. 1 (Jul 14 2021): 4319. https://doi.org/10.1038/s41467-021-24618-3.

Sauter, J. L., R. P. Graham, B. T. Larsen, S. M. Jenkins, A. C. Roden, and J. M. Boland. "Smarca4-Deficient Thoracic Sarcoma: A Distinctive Clinicopathological Entity with Undifferentiated Rhabdoid Morphology and Aggressive Behavior." [In eng]. *Mod Pathol* 30, no. 10 (Oct 2017): 1422-32. https://doi.org/10.1038/modpathol.2017.61.

Seo, J. S., Y. S. Ju, W. C. Lee, J. Y. Shin, J. K. Lee, T. Bleazard, J. Lee, *et al.* "The Transcriptional Landscape and Mutational Profile of Lung Adenocarcinoma." [In eng]. *Genome Res* 22, no. 11 (Nov 2012): 2109-19. https://doi.org/10.1101/gr.145144.112.

Stanton, B. Z., C. Hodges, J. P. Calarco, S. M. Braun, W. L. Ku, C. Kadoch, K. Zhao, and G. R. Crabtree. "Smarca4 Atpase Mutations Disrupt Direct Eviction of Prc1 from Chromatin." [In eng]. *Nat Genet* 49, no. 2 (Feb 2017): 282-88. https://doi.org/10.1038/ng.3735.

Tagal, V., S. Wei, W. Zhang, R. A. Brekken, B. A. Posner, M. Peyton, L. Girard, *et al.* "Smarca4-Inactivating Mutations Increase Sensitivity to Aurora Kinase a Inhibitor Vx-680 in Non-Small Cell Lung Cancers." [In eng]. *Nat Commun* 8 (Jan 19 2017): 14098. https://doi.org/10.1038/ncomms14098.

Truong, M. T., B. S. Sabloff, and J. P. Ko. "Multidetector Ct of Solitary Pulmonary Nodules." [In eng]. *Radiol Clin North Am* 48, no. 1 (Jan 2010): 141-55. https://doi.org/10.1016/j.rcl.2009.09.005.

van der Kaaij, R. T., F. E. M. Voncken, J. M. van Dieren, P. Snaebjornsson, C. M. Korse, C. Grootscholten, B. M. P. Aleman, and J. W. van Sandick. "Elevated Pretreatment Cea and Ca19-9 Levels Are Related to Early Treatment Failure in Esophageal Adenocarcinoma." [In eng]. *Am J Clin Oncol* 42, no. 4 (Apr 2019): 345-50. https://doi.org/10.1097/coc.0000000000000525.

Wong, A. K., F. Shanahan, Y. Chen, L. Lian, P. Ha, K. Hendricks, S. Ghaffari, *et al.* "Brg1, a Component of the Swi-Snf Complex, Is Mutated in Multiple Human Tumor Cell Lines." [In eng]. *Cancer Res* 60, no. 21 (Nov 1 2000): 6171-7.

Yamazaki, M., H. Ishikawa, R. Kunii, A. Tasaki, S. Sato, Y. Ikeda, N. Yoshimura, *et al.* "A Combination of Preoperative Ct Findings and Postoperative Serum Cea Levels Improves Recurrence Prediction for Stage I Lung Adenocarcinoma." [In eng]. *Eur J Radiol* 84, no. 1 (Jan 2015): 178-84. https://doi.org/10.1016/j.ejrad.2014.10.009.

Yang, Y., C. Shi, H. Sun, W. Yin, X. Zhou, L. Zhang, and G. Jiang. "Elderly Male Smokers with Right Lung Tumors Are Viable Candidates for Kras Mutation Screening." [In eng]. *Sci Rep* 6 (Jan 7 2016): 18566. https://doi.org/10.1038/srep18566.

Yoshida, A., E. Kobayashi, T. Kubo, M. Kodaira, T. Motoi, N. Motoi, K. Yonemori, *et al.* "Clinicopathological and Molecular Characterization of Smarca4-Deficient

Thoracic Sarcomas with Comparison to Potentially Related Entities." [In eng]. *Mod Pathol* 30, no. 6 (Jun 2017): 797–809. https://doi.org/10.1038/modpathol.2017.11.

Zerhouni, E. A., F. P. Stitik, S. S. Siegelman, D. P. Naidich, S. S. Sagel, A. V. Proto, J. R. Muhm, *et al*. "Ct of the Pulmonary Nodule: A Cooperative Study." [In eng]. *Radiology* 160, no. 2 (Aug 1986): 319–27. https://doi.org/10.1148/radiology.160.2.3726107.

Zwirewich, C. V., S. Vedal, R. R. Miller, and N. L. Müller. "Solitary Pulmonary Nodule: High–Resolution Ct and Radiologic–Pathologic Correlation." [In eng]. *Radiology* 179, no. 2 (May 1991): 469–76. https://doi.org/10.1148/radiology.179.2.2014294.

Funding

This research did not receive any specific grant from funding agencies in the public, commercial, or not-for-profit sectors.

Author information

The studies involving human participants were reviewed and approved by the Medical Ethical Committee of the Zhengzhou University. The patients/participants provided their written informed consent to participate in this study. Written informed consent was obtained from the individual(s) for the publication of any potentially identifiable images or data included in this article.

Author Contributions

Corresponding authors
Correspondence to Jianbo Gao

Ethics approval

The studies involving human participants were reviewed and approved by the Medical Ethical Committee of the Zhengzhou University. The patients/participants provided their written informed consent to participate in this study. Written informed consent was obtained from the individual(s) for the publication of any potentially identifiable images or data included in this article.

Consent to participate

Informed consent was obtained from all individual participants included in the study.

Consent to publish

The authors affirm that human research participants provided informed consent for publication of the images in Figure(s) 1, 2, 3, 4 and 5.

Conflict of interest

The authors declare that the research was conducted in the absence of any commercial or financial relationships that could be construed as a potential conflict of interest.

Fig. 1 SMARCA4-NSCLC in a 53-year-old man. (A B) Unenhanced CT image of lung reveals an intraluminal mass of homogeneous attenuation at the right upper lobe, with an irregular surface, contrast-enhanced CT image shows obvious inhomogeneous enhancement (C), with more obviously enhanced on the venous phase(D). Enlarged and significantly enhancement lymph nodes can be seen. Separately CT imaging at the position of coronal and sagittal (E F).

Fig. 2 A 63-year-old man: 99mTc-MDP SPECT shows pronounced tracer uptake in the sternum, the left scapula and the 4th rib left, the 5th rib right, T11 and the right sacroiliac joint. A small focal uptake posterior to the left orbital region.

Fig. 3 Histopathologic features of SMARCA4-deficient tumors(magnification, A 10×;B,C 20×;D 40×). Hematoxylin and eosin section showing the tumor cells arranged in nests with scant cytoplasm, obvious atypia, large nucleus with thickened nuclear membrane and granular chromatin. Mitoses and inflammatory cell infiltrate are frequent.

Fig. 4 SMARCA4-NSCLC, demonstrated complete lack of expression of SMARCA4(BRG1) in (A,B),with endothelial and inflammatory cells as internal positive controls. CK(C), and CK8/18 (D) showed intensive and diffuse expression. Scale bars are presented.

Figures

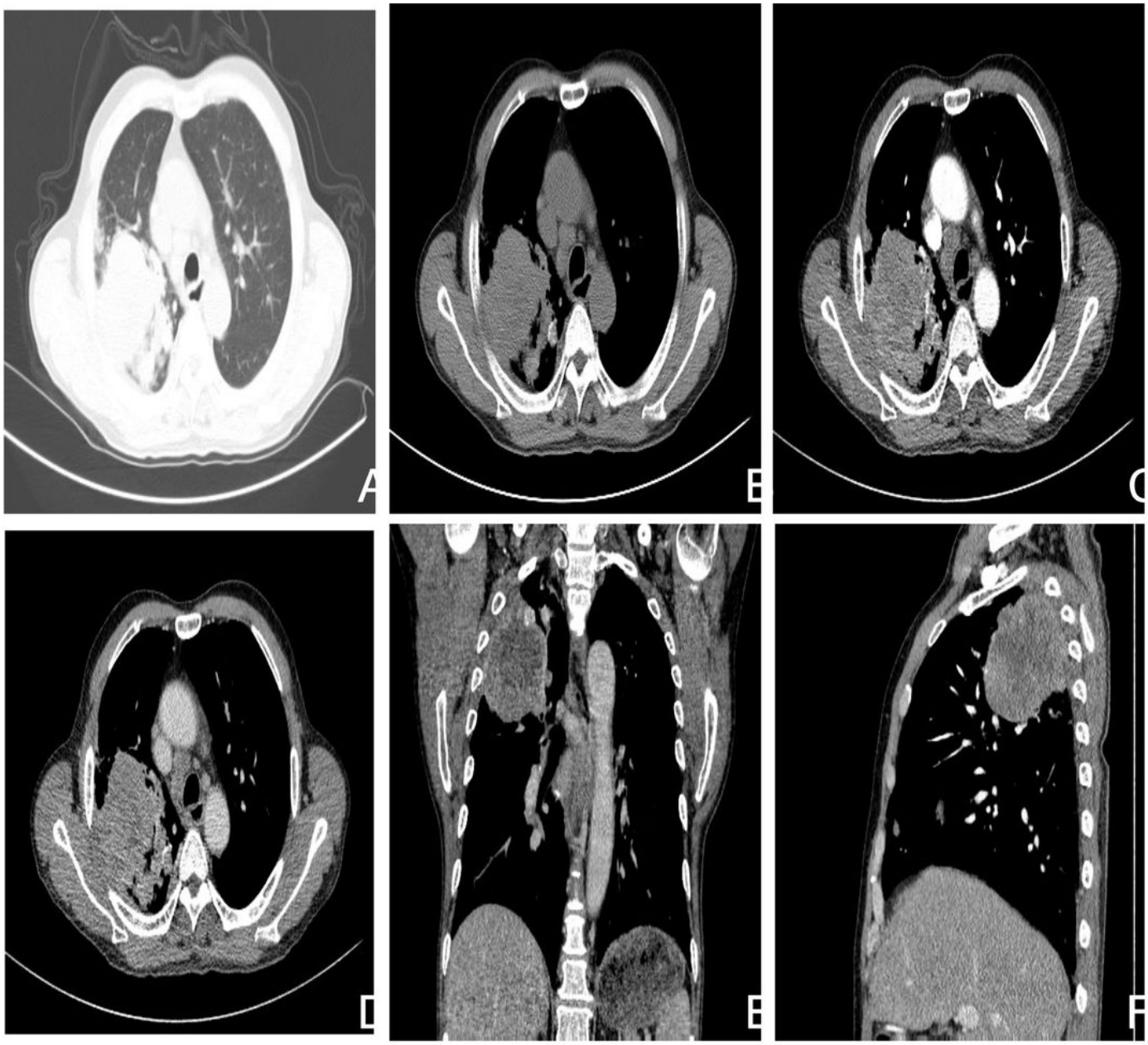

Fig. 1 SMARCA4-NSCLC in a 53-year-old man. (A B) Unenhanced CT image of lung reveals an intraluminal mass of homogeneous attenuation at the right upper lobe, with an irregular surface, contrast-enhanced CT image shows obvious inhomogeneous enhancement (C), with more obviously enhanced on the venous phase(D). Enlarged and significantly enhancement lymph nodes can be seen. Separately CT imaging at the position of coronal and sagittal (E F).

Figure 1

See image above for figure legend.

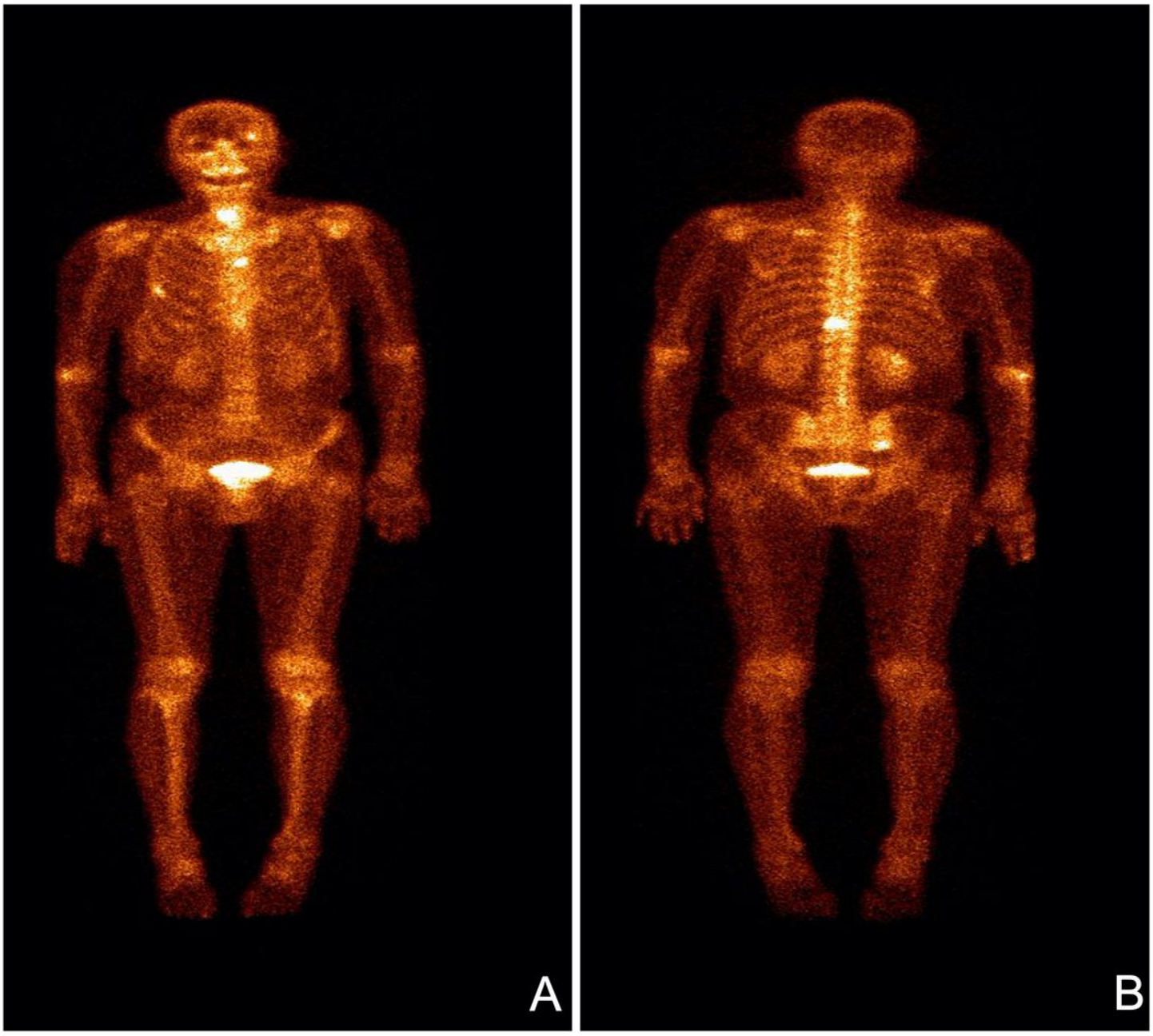

Fig. 2 A 63-year-old man: 99mTc-MDP SPECT shows pronounced tracer uptake in the sternum, the left scapula and the 4th rib left, the 5th rib right, T11 and the right sacroiliac joint. A small focal uptake posterior to the left orbital region.

Figure 2

See image above for figure legend.

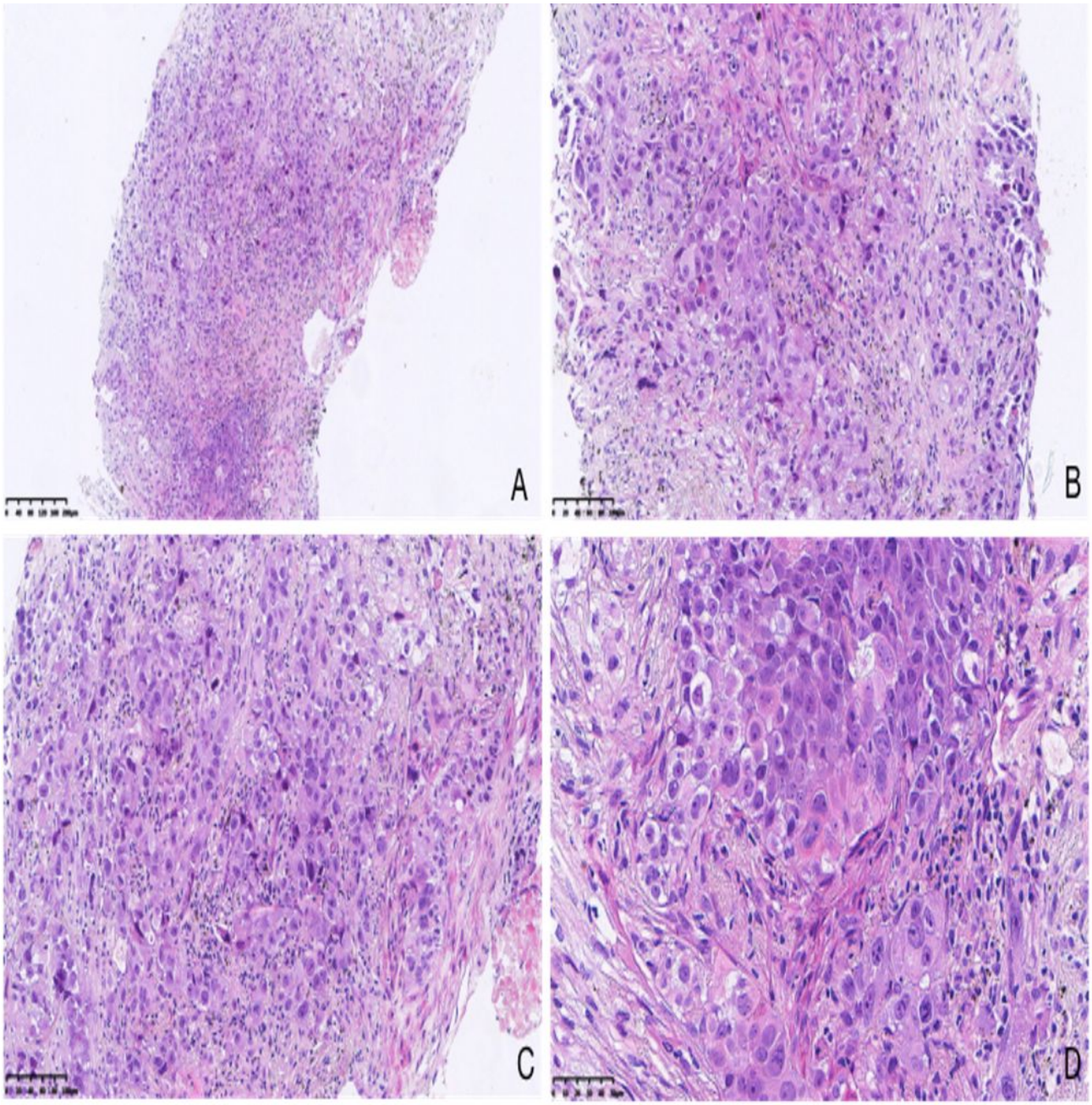

Fig. 3 Histopathologic features of SMARCA4-deficient tumors(magnification, A 10×;B,C 20×;D 40×). Hematoxylin and eosin section showing the tumor cells arranged in nests with scant cytoplasm, obvious atypia, large nucleus with thickened nuclear membrane and granular chromatin. Mitoses and inflammatory cell infiltrate are frequent.

Figure 3

See image above for figure legend.

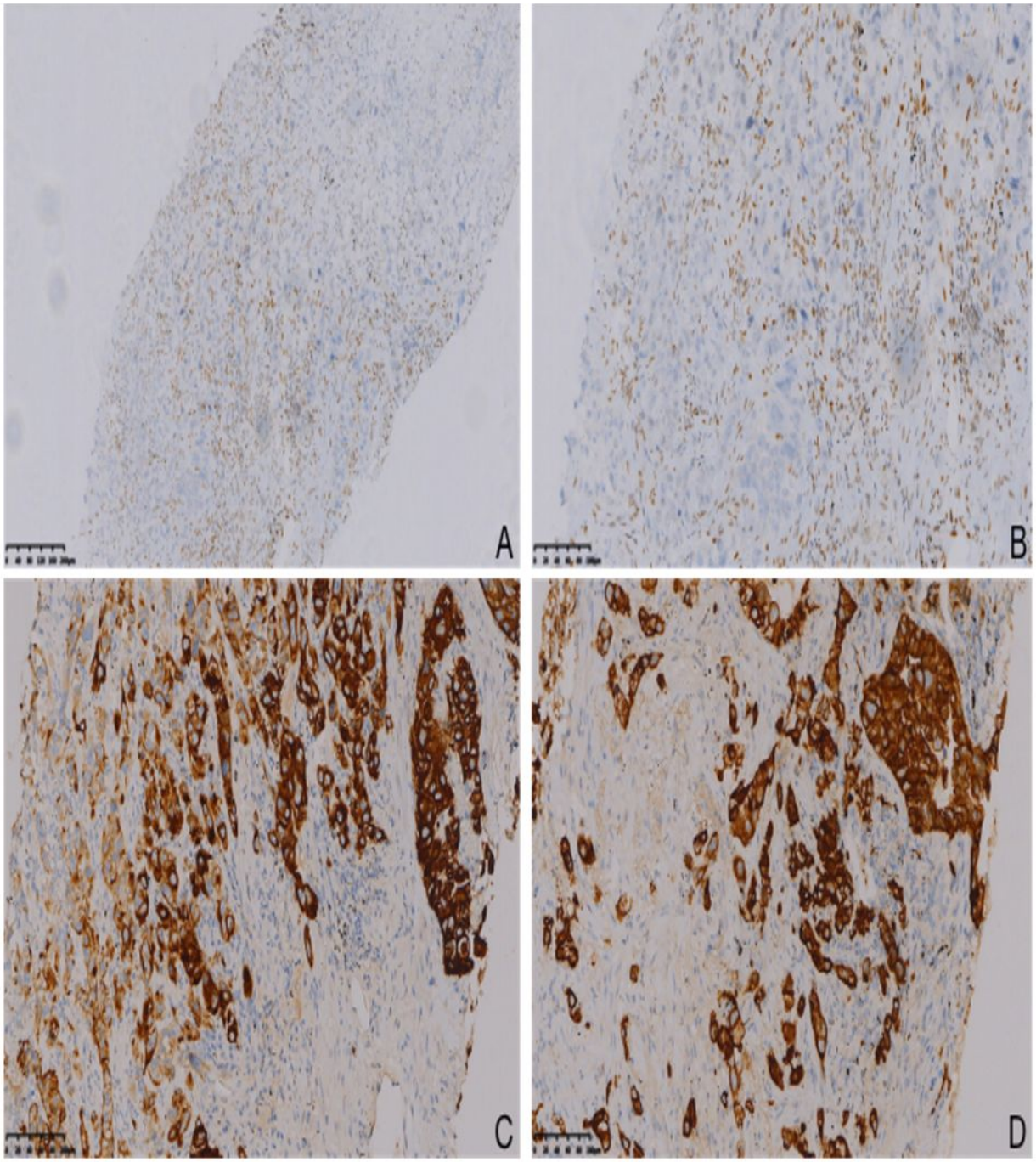

Fig. 4 SMARCA4-NSCLC, demonstrated complete lack of expression of SMARCA4(BRG1) in (A,B),with endothelial and inflammatory cells as internal positive controls. CK(C), and CK8/18 (D) showed intensive and diffuse expression. Scale bars are presented.

Figure 4

See image above for figure legend.

Supplementary Files

This is a list of supplementary files associated with this preprint. Click to download.

- APPENDIXTable.docx